Fluorosurfactant Self-Assembly at Solid/Liquid Interfaces

Orlando J. Rojas,*[,†,‡] Lubica Macakova,[‡] Eva Blomberg,[‡,§] Åsa Emmer,[⊥] and Per M. Claesson[‡,§]

Escuela de Ingeniería Química, Lab. FIRP, Universidad de Los Andes, Mérida 5101, Venezuela, Department of Chemistry, Surface Chemistry, Drottning Kristinas väg 51, Royal Institute of Technology, SE-100 44 Stockholm, Sweden, Institute for Surface Chemistry, Box 5607, SE-114 86 Stockholm, Sweden, and Department of Chemistry, Analytical Chemistry, Royal Institute of Technology, SE-100 44 Stockholm, Sweden

Received May 25, 2002. In Final Form: July 26, 2002

Fluorosurfactants have some unique properties that are advantageously used in a range of applications. Their solutions are commonly in contact with solid surfaces onto which the molecules adsorb. Despite this, the adsorption behavior of fluorosurfactants at solid/liquid interfaces is not sufficiently understood, and there is a need for more information. In this study we focus on cationic fluorosurfactant adsorption on negatively charged hydrophilic surfaces, especially with respect to the adsorbed layer structure, long-range interactions, and adhesion forces. To this end we combined results obtained from bimorph and interferometric surface force instruments and ellipsometry techniques. The initial adsorption to the oppositely charged surfaces occurs due to the electrostatic attraction between the charged headgroups and the surface. Further adsorption, driven by hydrophobic interactions, occurs readily as the surfactant concentration is increased. Surface force and ellipsometric experiments indicate that the surfactants self-assemble in the form of bilayer aggregates. The thickness of the bilayer aggregates was found to be consistent with the molecular structure. Further, ellipsometric measurements indicate that no complete bilayers were formed but rather that bilayer aggregates were present on the surface even at concentrations well above the cmc. Surface force data for low fluorosurfactant concentrations demonstrate that upon compression the bilayer aggregates assembled on the isolated surfaces are transformed, and as a result monolayer structures build up between the surfaces in contact. The force required to attain bilayer−bilayer contact increases with the surfactant bulk concentration due to an increase in the repulsive double-layer force. The force required to drive out surfactant molecules to achieve monolayer−monolayer contact also increases with surfactant concentration. Above the cmc some additional aggregates are present on top of the bilayer aggregates coating the surface. The adhesion found between the monolayer aggregates is an order of magnitude larger than between the bilayer aggregates. However, it is an order of magnitude lower than the corresponding value for Langmuir−Blodgett monolayer films of similar fluorosurfactants.

Introduction

The synthesis and bulk behavior of fluorinated amphiphiles have been the subject of many investigations, some of which have been reviewed recently.[1] One of the reasons for the current interest stems from the unique properties exhibited by fluorocarbons. Fluorocarbons substantially surpass hydrocarbons in terms of thermal, chemical, and biological inertness, surface activity (both effectiveness and efficiency), gas dissolving capacity, hydrophobicity, and lipophobicity. The remarkably strong intramolecular bonds and characteristic intermolecular interactions are the origin of some of these properties. This also results in low surface tension, high fluidity, excellent spreading characteristics, low solubility in water, and high density, all of which are the basis for innovative applications in different fields, especially in biomedicine.[2−9]

The interrogation of adsorption layers on an overflowing cylinder (OFC) cell using ellipsometry, surface-light scattering, laser Doppler velocimetry, and neutron reflection has been explored.[10−12] Studies at the gas/liquid interface regarding to packing and coverage of fluorosurfactants have been undertaken using X-ray reflectivity.[13]

The modification of solid surface characteristics brought about by adsorption of fluorosurfactants has been used in various analytical applications. Fluorosurfactants are being used as additive in buffer solutions for (free-flow) capillary electrophoretic separation of proteins, peptides, and enzymes,[14−18] in micellar electrokinetic chromatography (MEKC),[19,20] and in obtaining peptide maps by

† Universidad de Los Andes.
‡ Surface Chemistry, Royal Institute of Technology.
§ Institute for Surface Chemistry.
⊥ Analytical Chemistry, Royal Institute of Technology.
* Corresponding author.

(1) Abe, M. *Curr. Opin. Colloid Interface Sci.* **1999**, *4*, 354.
(2) Reuter, P.; Meinert, H. *J. Fluorine Chem.* **1991**, *54*, 185.
(3) Krafft, M. P.; Riess, J. G. *Biochimie* **1998**, *80*, 489.
(4) Riess, J. G.; Krafft, M. P. *Biomaterials* **1998**, *19*, 1529.
(5) Nivet, J. B.; LeBlanc, M.; Riess, J. G. *J. Fluorine Chem.* **1992**, *58*, 210.
(6) Krafft, M. P. *Adv. Drug Delivery Rev.* **2001**, *47*, 209.
(7) Northoff, H.; Haidmann, L.; Hänsch, G.; Reuter, P.; Mader, J.; Meinert, H. *Infusionstherapie Und Transfusionsmedizin* **1992**, *19*, 115.
(8) Riess, J. G. *New J. Chem.* **1995**, *19*, 891.
(9) Vierling, P.; Santaella, C.; Greiner, J. *J. Fluorine Chem.* **2001**, *107*, 337.
(10) Eastoe, J.; Nave, S.; Downer, A.; Paul, A.; Rankin, A.; Tribe, K.; Penfold, J. *Langmuir* **2000**, *16*, 4511.
(11) Eastoe, J.; Rankin, A.; Wat, R.; Bain, C. D. *Int. Rev. Phys. Chem.* **2001**, *20*, 357.
(12) Eastoe, J.; Paul, A.; Rankin, A.; Wat, R.; Penfold, J.; Webster, J. R. P. *Langmuir* **2001**, *17*, 7873.
(13) Zou, X.; Barton, S. W. *Langmuir* **1994**, *10*, 2866.
(14) Emmer, Å.; Jansson, M.; Roeraade, J. *J. Chromatogr.* **1991**, *547*, 544.
(15) Emmer, Å.; Jansson, M.; Roeraade, J. *J. Chromatogr. A* **1994**, *672*, 231.
(16) Emmer, Å.; Roeraade, J. *J. Liq. Chromatogr.* **1994**, *17*, 3831.
(17) Hult, E. L.; Emmer, Å.; Roeraade, J. *J. Chromatogr. A* **1997**, *757*, 255.
(18) Sjödahl, J.; Emmer, Å.; Karlstam, B.; Vincent, J.; Roeraade, J. *J. Chromatogr. B* **1998**, *705*, 231.
(19) Yang, S.; Khaledi, M. G. *Anal. Chem.* **1995**, *67*, 499.

10.1021/la025989c CCC: $22.00
Published on Web 09/04/2002

performing tryptic digests in chip-based open vials.[21] Fluorosurfactants are also used to change the hydrophobicity of a solid surface in applications concerning the use of fluorocarbon-based technologies for biomolecule separation and immobilization, heterogeneous diagnostic assays, and preparation of biosensors.[22,23]

In capillary electrophoresis it is hypothesized that the formation of a fluorosurfactant bilayer at the silica capillary inner wall allows the adjustment of the surface charge (wall deactivation)[24] and thus permits the reduction of protein adsorption to the capillary wall at a pH below their pI.[14] The separation performance and selectivity can be further improved by using mixtures of different types of fluorosurfactants in the running buffer, making it possible to separate both positively and negatively charged proteins in the same run without having to change the buffer strength or pH.[15−17] In this case the magnitude and direction of the electroosmotic flow are tailored by the composition of the surfactant mixture, and a model has been forwarded to explain this behavior in terms of micellation and formation of admicellar surfactant layers.[17]

Studies on direct adsorption of fluorosurfactants on solid surfaces are very scarce. The adsorption of cationic fluorosurfactants on mica[25] and on aluminum oxide[26] surfaces has been studied experimentally. Contact angle and wettability measurements have been used to investigate adsorption on powdered dyes[27] and on low-energy solids.[28] Contact angles and friction coefficients for adsorbed films of surfactant on alumina chips were studied as a function of pH and surfactant concentration.[26] The adsorbed layer structure of partially fluorinated cationic surfactants and their mixtures on mica were determined by AFM imaging. It was indicated that the fluorosurfactant self-assembled as cylindrical micelles and shape transitions in the adsorbed layer were correlated with surface and bulk compositions.[29]

Interaction forces between adsorbed layers of fluorosurfactants in aqueous solution have been investigated with the aim of unveiling the nature of the "hydrophobic" interaction. Most of the measurements have been performed using Langmuir−Blodgett (LB) films and solids modified with reactive fluorocarbon/silane molecules.[30,31] The phase separation and orientation of molecules in mixed LB films of hydrocarbon and fluorocarbon amphiphilic compounds have been studied using scanning surface potential microscopy, AFM, and friction force microscopy.[32−34]

Friction and adhesion hysteresis experiments were carried out on fluorocarbon surfactant monolayer-coated surfaces using the surface forces apparatus (SFA).[35] In these cases the SFA and the interfacial gauge (IG)[36,37] were employed. The tribological properties of highly ordered self-assembled monolayers of fluorocarbon and hydrocarbon thiols and disulfides formed on gold were studied by scanning force microscopy.[38]

Long-range hydrophobic interactions have additionally been studied on other solid substrates. Hydrophobic surfaces produced with fluorinated acids adsorbed/reacted on alumina from aqueous solution were investigated using classical adsorption isotherms, contact angle measurements, and colloid probe atomic force microscopy.[39] Self-assembled monolayers of semifluorinated alkanethiols on gold have been examined by direct force measurements in aqueous solutions.[40] The structure of similar systems has also been investigated with AFM, X-ray photoelectron spectroscopy (XPS), and surface plasmon resonance spectroscopy.[41]

Layers of fluorosilane moieties grown on silicon surfaces were characterized by ellipsometry. The hydrophobic surfaces obtained were also examined by AFM (in water), showing that the area occupied by fluorocarbon chains is 15% larger than that of hydrocarbon chains.[42] The attraction between hydrophobized silica surfaces was also studied by using an AFM-related force-measuring device.[43]

Interaction force studies are not restricted to aqueous systems. Force measurements between two fluorocarbon surfactant monolayers adsorbed from ethylene glycol solutions were accomplished.[44] AFM was also used to measure the force of interaction between a micron-sized colloidal sphere and a flat plate coated with fluoropolymers in water and other organic solvents.[45]

It is apparent that the published investigations on interaction forces of fluorocarbon surfaces have been aimed at exploring the nature of solvophobic effects. On the other hand, little attention has been paid to the adsorbed layer structure on the solid surface and its dependence on the bulk surfactant concentration.

Claesson and Christenson[46] reported the first investigation on interaction forces between fluorosurfactants layers obtained by LB deposition on mica as measured by the SFA. It was indicated that a weakly adsorbed second layer could be a reason for previously observed lower hydrophobic attraction between adsorbed hydrocarbon surfactants. The same group investigated the effect of salts on the hydrophobic interaction forces between fluorosurfactants adsorbed from bulk solution on mica.[47]

(20) de Ridder, R.; Damin, F.; Reijenga, J.; Chiari, M. *J. Chromatogr. A* **2001**, *916*, 73.
(21) Litborn, E.; Emmer, Å.; Roeraade, J. *Anal. Chim. Acta* **1999**, 401.
(22) Boivin, P.; Kobos, R. K.; Papa, S. L.; Scouten, W. H. *Biotechnol. Appl. Biochem.* **1991**, *14*, 155.
(23) Arentzen, R.; Jadhav, P. K.; Kobos, R.; Smart, B. *Biotechnol. Adv.* **1997**, *15*, 172.
(24) Emmer, Å.; Roeraade, J. *Electrophoresis* **2001**, *22*, 660.
(25) Herder, P. C.; Claesson, P. M.; Herder, C. E. *J. Colloid Interface Sci.* **1987**, *119*, 155.
(26) Lai, C. L.; Harwell, J. H.; Orear, E. A.; Komatsuzaki, S.; Arai, J.; Nakakawaji, T.; Ito, Y. *Colloids Surf., A* **1995**, *104*, 231.
(27) Hartmann, G. *Colloids Surf.* **1991**, *57*, 205.
(28) Mukerjee, P. *Colloids Surf., A* **1994**, *84*, 1.
(29) Davey, T. W.; Warr, G. G.; Almgren, M.; Asakawa, T. *Langmuir* **2001**, *17*, 5283.
(30) Ohnishi, S.; Yaminsky, V. V.; Christenson, H. K. *Langmuir* **2000**, *16*, 8360.
(31) Ohnishi, S.; Ishida, T.; Yaminsky, V.; Christenson, H. K. *Langmuir* **2000**, *16*, 2722.
(32) Zhu, B. Y.; Zhang, P.; Wang, L.; Liu, Z. F. *J. Colloid Interface Sci.* **1997**, *185*, 551.
(33) Yagi, K.; Fujihira, M. *Appl. Surf. Sci.* **2000**, *157*, 405.
(34) Imae, T.; Takeshita, T.; Kato, M. *Langmuir* **2000**, *16*, 612.
(35) Yamada, S.; Israelachvili, J. *J. Phys. Chem. B* **1998**, *102*, 234.
(36) Yaminsky, V. V.; Jones, C.; Yaminsky, F.; Ninham, B. *Langmuir* **1996**, *12*, 3531.
(37) Yaminsky, V. V.; Ninham, B. W.; Stewart, A. M. *Langmuir* **1996**, *12*, 836.
(38) Schonherr, H.; Vancso, G. J. *Mater. Sci. Eng., C* **1999**, *8−9*, 243.
(39) Karaman, M. E.; Antelmi, D. A.; Pashley, R. M. *Colloids Surf. A* **2001**, *182*, 285.
(40) Ederth, T.; Tamada, K.; Claesson, P. M.; Valiokas, R.; Colorado, R.; Graupe, M.; Shmakova, O. E.; Lee, T. R. *J. Colloid Interface Sci.* **2001**, *235*, 391.
(41) Tamada, K.; Ishida, T.; Knoll, W.; Fukushima, H.; Colorado, R.; Graupe, M.; Shmakova, O. E.; Lee, T. R. *Langmuir* **2001**, *17*, 1913.
(42) Fujii, M.; Sugisawa, S.; Fukada, K.; Kato, T.; Shirakawa, T.; Seimiya, T. *Langmuir* **1994**, *10*, 984.
(43) Yakubov, G. E.; Butt, H. J.; Vinogradova, O. I. *J. Phys. Chem. B* **2000**, *104*, 3407.
(44) Parker, J. L.; Claesson, P. M. *Langmuir* **1992**, *8*, 757.
(45) Considine, R. F.; Drummond, C. J. *Langmuir* **2000**, *16*, 631.
(46) Claesson, P. M.; Christenson, H. K. *J. Phys. Chem.* **1988**, *92*, 1650.
(47) Christenson, H. K.; Claesson, P. M.; Berg, J.; Herder, P. C. *J. Phys. Chem.* **1989**, *93*, 1472.

Most of the reported studies deal with ways to synthesize and characterize fluorocarbons and fluorinated amphiphiles. However, despite its relevance, it is evident that studies on fluorosurfactant self-assembly on solid surfaces are limited. There is a need to strengthen the research on supramolecular assemblies and the correlation between molecular structure and surface physical properties. In this study we report on the adsorption behavior and interaction forces of fluorosurfactants adsorbed on solid surfaces at various concentrations as studied by ellipsometry, surface force, and complementary techniques.

Experimental Section

Materials and Methods. The fluorosurfactant used in this study was the same as employed in previous investigations on capillary electrophoresis and tryptic digests in chip-based vials.[17,21] It is a quaternary ammonium iodide salt of perfluorooctanesulfonamide obtained from 3M Co. (St. Paul, MN), trade name fc-134 (note that this product is no longer commercially available). The fluorosurfactant sample is polydisperse as confirmed by results from MALDI-MS experiments that showed that C8F17 is the dominating fluorocarbon tail ($CF_3-(CF_2)_7-SO_2-NH-(CH_2)_3-N^+(CH_3)_3\ I^-$), but fluorosurfactants with C7F15, C6F13, C5F11, and C4F9 chains are also present.

Water used in all the experiments was first purified by a reverse osmosis unit (Milli-RO 10 Plus), which includes depth filtration, carbon adsorption, and decalcination. A Milli-Q Plus 185 unit was then used to treat the water with UV light and with a Q-PAK unit consisting of an activated carbon column, a mixed-bed ion exchanger, and an Organex cartridge with a final 0.22 μm Millipack 40 filter. The fluorosurfactant was dissolved in Milli-Q water and made up to stock solutions with a concentration of 500 μg/mL. Aqueous solution of sodium iodide (0.1 mM, pro-analysis grade, from Merck) was employed throughout the work as background electrolyte.

Ellipsometry. The experimental setup and methodology employed, namely multiple-media in-situ ellipsometry, are thoroughly explained in refs 48 and 49. In brief, the measurements were conducted with a Multiscop (Optrel GBR, Berlin, Germany) ellipsometer equipped with a Nd:YAG laser with a wavelength of 532 nm. As substrate, polished silicon wafers with an approximately 30 nm thick layer of thermally grown SiO_2 were used. The wafers were cut to 3 × 1 cm slides, which were then cleaned in two steps at 80 °C and for 10 min each. The first cleaning solution consisted of 25% NH_3, 30% H_2O_2, and H_2O (1:1:5 by volume) and the second one of a mixture consisting of 30% HCl, 30% H_2O_2, and H_2O (1:1:5). After cleaning, the slides were extensively rinsed with Milli-Q water and stored in ethanol until used. Prior to any experiment, the slides were exposed to plasma (Harrick, PDC 2XG) for 5 min to remove any contaminants that could remain on the surface.

All measurements were performed at an angle of incidence of 67.34°, in a trapezoidal quartz cuvette thermostated to 25 °C. The content of the cuvette was continuously stirred with a magnetic stirrer operated at 300 rpm. The desired concentrations were achieved by stepwise addition into the cuvette of the appropriate volume of a 500 μg/mL stock solution of fluorosurfactant in 0.1 mM NaI background electrolyte. The solution was filtered through a 0.2 μm PTFE filter prior to injection in order to abide by the procedure followed in MASIF experiments.

At first, the optical properties of the substrate were ascertained by four zone measurements of the ellipsometric angles (Ψ and Δ) in air and in aqueous 0.1 mM NaI solution. The calculated values of the complex refractive index of Si and the thickness and the refractive index of SiO_2 were used as input parameters in the model for calculation of the thickness (d_f) and refractive index (n_f) of the adsorbed surfactant layer. In the calculation a four-layer model (Si, SiO_2, adsorbed layer, and electrolyte) was employed, assuming planar interfaces and isotropic media.

During the process of adsorption, Ψ and Δ were measured in one zone only. However, four zone measurements were done for every particular concentration of fluorosurfactants after the adsorption reached equilibrium. Thus, the correct values of Ψ and Δ could be obtained in one zone by employing linear correction factors.

The adsorbed amount (Γ) was calculated according to the de Feijter equation:[50]

$$\Gamma = \frac{n_f - n_0}{dn/dc} d_f$$

where n_0 is refractive index of the electrolyte solution and dn/dc is the refractive index increment for the surfactant solution. The refractive index increment for the surfactant solution was determined to be 0.071 cm^3/g using an Optilab DSP interferometric refractometer (Wyatt Technology, Santa Barbara, CA).

Surface Interaction Forces. Force measurements were conducted using the noninterferometric surface force apparatus developed by Parker.[51−53] This device, commonly known as MASIF (measurements and analysis of surface interactions and forces), employs a bimorph force/deflection sensor that after calibration yields the interaction force. One of the surfaces (bottom surface) is mounted on the edge of the bimorph and the other (the top one) at the end of a piezoelectric tube. The assembly is enclosed in a stainless steel cell of ca. 10 mL volume and mounted on a translation stage that is isolated form electrical and sound noise. During a typical force measurement, the surfaces are driven closer (and then farther apart) by applying a triangular voltage wave to the piezo crystal. Simultaneously, the charge produced upon any deflection of the bimorph, due to repulsive or attractive forces, is recorded. Once the surfaces come into hard-wall contact, the linear movement of the piezo deflects the bimorph, thus enabling the force sensor to be calibrated against the known piezo crystal expansion and contraction as measured by a linear variable differential transformer (LVDT) sensor. Provided the deflection and the spring constant of the bimorph are known, the data are used to calculate the force−distance curves from Hooke's law. The noninterferometric surface force apparatus does not allow absolute determination of the zero surface separation. In our case the layer thickness was obtained from the magnitude of the inward "jump" that occurs when a surfactant layer is pushed out from the contact area upon compression.

It has been shown[54] that flame-polished glass surfaces are smooth enough to enable accurate measurements of surface forces down to molecular separations. The surfaces used in each experiment were prepared by melting one end of a borosilicate glass rod (diameter 2 mm, length ca. 25 mm) in a butane−oxygen burner until the tip formed into as a sphere with a diameter of about 4 mm. The normal radii of curvature (r_1 and r_2) for each surface were determined more accurately at the end of the experiment by using a micrometer, and the local harmonic mean radius of the interaction, R, was then calculated as $R = 2r_1r_2/(r_1 + r_2)$. The spring constant of the bimorph was measured at the end of each experiment by placing known weights on the bimorph spring and measuring the resulting deflection (usually about 100 N/m). The force was then normalized by the local harmonic mean radius of interaction (F/R).

All procedures for assembling the measuring chamber and preparing the solutions were carried out inside a laminar flow cabinet. At the beginning of each set of experiments, the interaction profiles were first determined in air to ensure that the system showed no signs of contamination. Following, the 0.1 mM sodium iodide solution (background electrolyte) was introduced into the measuring chamber, and interaction profiles were again determined. Concentrated stock surfactant solution was then introduced through a 0.2 μm PTFE filter until the desired concentration inside the chamber was attained. In experiments

(48) Landgren, M.; Jönsson, B. *J. Phys. Chem.* **1993**, *97*, 1656.
(49) Tiberg, F.; Landgren, M. *Langmuir* **1993**, *9*, 927.
(50) de Feijter, J. A.; Benjamins, J.; Veer, F. A. *Biopolymers* **1978**, *17*, 1759.
(51) Parker, J. L. *Prog. Surf. Sci.* **1994**, *47*, 205.
(52) Parker, J. L.; Christenson, H. K.; Ninham, B. W. *Rev. Sci. Instrum.* **1989**, *60*, 3135.
(53) Parker, J. L.; Claesson, P. M. *Langmuir* **1994**, *10*, 635.
(54) Ederth, T.; Claesson, P. M.; Lindberg, B. *Langmuir* **1998**, *14*, 4782.

where the surfactant concentration was consecutively varied, part of the volume of the chamber was drained and then replaced with a surfactant solution of appropriate composition. Thus, in these measurements, each new concentration adsorbs to a surface preequilibrated with the previous solution and not to a bare surface.

The measured forces were analyzed using classical Derjaguin–Landau–Verwey–Overbeek theory[55,56] taking into account double-layer forces and attractive van der Waals forces. The double-layer force was calculated within the nonlinear Poisson–Boltzmann model, using constant surface charge boundary conditions, because these generally better approximated the measured forces than those calculated at constant potential. The van der Waals force between the surfactant-coated interfaces can be accurately calculated using a three-layer model (surface–surfactant layer–solvent).[57] However, the ellipsometric measurements to be presented below show that the refractive index of the adsorbed layer (1.42) is only marginally lower than that of silica (and glass). Hence, we have chosen to use the value of the nonretarded Hamaker constant for quartz–water–quartz (0.7×10^{-20} J) in all calculations.

Some comparisons between measurements from the MASIF and the interferometric surface force apparatus (SFA, model Mark IV) are reported herein, and the reader is referred to accounts on the SFA technique for a detailed description.[52,58] Suffice it to say that in this technique two molecularly smooth surfaces of freshly cleaved mica are used as substrate, and the surface interaction forces are measured with a double cantilever leaf spring. The separation between the two surfaces (in the range of microns down to molecular contact) is measured by multiple beam interferometry. The interaction force is obtained by expanding or contracting the piezoelectric crystal by a known amount and then measuring optically how much the two surfaces have actually moved. The measured force between crossed cylinders is normalized by the local geometric mean radius.

We note that the SFA technique allows direct measurement of the adsorbed layer thickness. The MASIF and SFA techniques use macroscopic surfaces with a radius of about 2 and 20 mm, respectively. The radius of curvature is in both cases too large to result in any curvature effects on the adsorbed layer structure. All measurements were carried out at 22 ± 1 °C.

Complementary Techniques. To discuss the role of the aggregation phenomenon in bulk solution the critical micelle concentration (cmc) was determined for fluorosurfactant in aqueous 0.1 mM NaI solution. The surface tension was determined by the ring method using a Sigma 70 system (KSV Instruments Ltd., Helsinki, Finland). The zero contact angle between the ring and the solution was achieved by cleaning the ring in a butane flame for 30 s prior to each measurement. A cmc equivalent to a fluorosurfactant concentration of 30 μg/mL in aqueous 0.1 mM NaI solution was obtained.

Results and Discussion

Ellipsometry. The adsorption kinetics was followed by ellipsometry. Figure 1a illustrates the ellipsometric adsorbed amount, Γ, as a function of the elapsed time after stepwise addition of the investigated fluorosurfactant under conditions similar as those employed in the force measurements to be presented later, i.e., at surfactant concentrations from 2 to 100 μg/mL in aqueous 0.1 mM NaI solution. The equilibrium adsorption isotherm, i.e., the adsorbed amount as a function of surfactant concentration, is also shown in Figure 1b. Table 1 includes the calculated ellipsometric layer thickness, refractive index, and the adsorbed amount per unit area.

The initial values of the adsorbed amount (= 0) shown in Figure 1a represent the case of surfactant-free solution, i.e., aqueous 0.1 mM NaI. After addition of surfactant up to a concentration of 2 μg/mL, it can be realized that a limited adsorption takes place. The equilibrium is reached very fast, and ca. 0.1 mg/m^2 adsorbed amount is observed. The corresponding layer thickness is negligible compared to the corresponding value for higher concentrations (2.5–4 nm). It can thus be inferred that at this stage much less than an adsorbed monolayer is formed, and the surfactant molecules most probably lie flat or nearly flat on the solid surface. As indicated by the force measurements (to be discussed later), little changes occur in the system at this low concentration except for a partial neutralization of surface charges and reduction in the short-range repulsion.

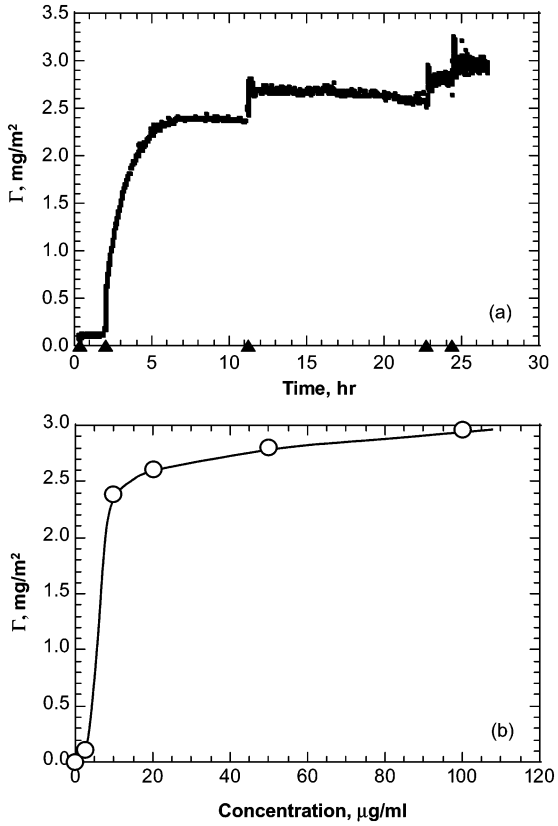

Figure 1. (a) Ellipsometric adsorbed amount after stepwise addition of fluorosurfactant solution to a silica surface. The black arrows indicate the time of addition for total fluorosurfactant concentrations in the cuvette of 2, 10, 20, 50, and 100 μg/mL. The zero level corresponds to a baseline of aqueous 0.1 mM NaI solution (pH = 5.6). (b) Adsorption isotherm for equilibrium adsorbed amount of fluorosurfactants on silica at different concentrations.

Table 1. Properties of Adsorbed Layers As Determined by Ellipsometric Measurements upon Equilibrium Adsorption of Cationic Fluorosurfactant on Silica in Aqueous 0.1 mM NaI Solution[a]

concn, μg/mL	ellipsometric thickness (d_f), nm	refractive index (n_f)	adsorbed amount (Γ), mg/m^2	average area/molecule, Å^2
0	0	1.33	0	
2			0.11	1095
10	3–4	1.38	2.34	103
20	3	1.37	2.61	92.4
50	2.7	1.40	2.74	88
100	2.5	1.41	2.88	83.8

[a] The average area per molecule calculated for 10, 20, 50, and 100 μg/mL surfactant concentrations is based on the assumption of a homogeneous bilayer structure and the average composition of the surfactant.

(55) Derjaguin, B.; Landau, L. *Acta Physiochem.* **1941**, *14*, 633.
(56) Verwey, E. G. W.; Overbeek, J. T. G. *The Theory of the Stability of Liophobic Colloids*; Elsevier: Amsterdam, 1948.
(57) Ninham, B. W.; Parsegian, V. A. *J. Chem. Phys.* **1970**, *52*, 4578.
(58) Israelachvili, J. N.; Adams, G. E. *J. Chem. Soc., Faraday Trans. 1* **1978**, *74*, 975.

A distinctive increment in the adsorbed amount was observed after increasing the concentration of fluorosurfactant in solution up to 10 μg/mL. The adsorption dynamics follows a two-step mechanism, which in the first stage consists of a rapid adsorption process followed by a considerably slower adsorption process, and equilibrium is not reached until after ca. 5 h. It is at this concentration where force measurements showed that the incubation time affects the surface interaction profile (and the layer structure). Bilayer structures with a thickness of about 3−4 nm are formed 1 h after surfactant addition. The low average refractive index of the layer (1.38) and the corresponding adsorbed amount at this time indicates loosely packed bilayer aggregates.

Later on, when equilibrium is reached, the adsorbed amount is increased (doubled), indicating an increase in the surface density of the adsorbed bilayer structures. The layer thickness rises to above 3 nm and the refractive index decreases slightly, indicating a layer of low density that, as demonstrated by the force measurements (to be presented later), is easy to squeeze away by applying high loads. The structure of the bilayer surface aggregates is likely to be affected by electrostatic and hydrophobic interactions. The electrostatic attraction between the surfactant cationic groups and the anionic surface provides the driving force for the attachment to the surface. The hydrophobic interactions between the fluorosurfactant tails promote formation of bilayer aggregates, and the electrostatic repulsion between the headgroups not in contact with the surface favors formation of small bilayer aggregates over complete bilayers. The detailed structure of the surface aggregates is not known yet, and we have chosen to call these structures "bilayer aggregates". A more detailed study of this issue is advanced by the interaction force study.

After addition of surfactants up to 20 μg/mL a small but rapid increase of the adsorbed amount (to 2.6 mg/m^2) was observed. Additional surfactant molecules are incorporated into the structure. The layer thickness is reduced to 3 nm, and the refractive index rises up to 1.40. This behavior indicates that a more tight packing of the molecules within the bilayer is attained.

Further increase of the surfactant concentration up to 100 μg/mL did not cause any dramatic change in the layer quality. A relatively small increase of the adsorbed amount to a final value of 2.9 mg/m^2 was observed. This change was accompanied by a marginal reduction of the layer thickness to 2.5−3 nm and an increase of the refractive index to 1.42. It can be envisioned that at a molecular level the bilayer aggregates pack closer together to the surface. For surfactant concentrations of 50 and 100 μg/mL, variations in the ellipsometric angles were observed, and therefore the calculated adsorbed amount, refractive index, and layer thickness showed some instability. This can be explained by the effect of thermal and concentration gradients occurring in the vicinity of the surface (which produce large changes in the calculated values) and formation of fluorosurfactants aggregates in the bulk solution that adsorb and desorb from the surface.

The calculated area per molecule assuming homogeneous bilayer coverage is between 103 Å^2 (10 μg/mL) and 83 Å^2 (100 μg/mL) (see Table 1). However, the corresponding figure for the actual area per headgroup within a bilayer aggregate should be different (lower) since, as indicated before, the adsorption of fluorosurfactant occurs in the form of patchy bilayer aggregates. As a reference, it should be noted that the physical cross-sectional area of a fluorocarbon chain is approximately 28 Å^2,[59] and areas per molecule of the order of 56−78 Å^2 in densely packed monolayers at air/liquid interfaces have been reported for various fluorosurfactants.[10,12,60]

An unexpected observation is the reduction of the ellipsometric thickness (accompanied by an increase in the refractive index) as the fluorosurfactant concentration is increased (see Table 1). This phenomenon was corroborated in repeated ellipsometric measurements that consistently showed the same trend. We hypothesize that this effect is due to the polydispersity in the chain length of the fluorosurfactant molecules. In fact, the studied fluorosurfactant is not monodisperse since in the manufacturing process the fluorocarbon chain does not have a unique length but rather a limited size distribution. As such, we propose that initially (at low surfactant concentrations) longer-chain molecules are preferentially adsorbed on the solid surface, and thicker bilayer aggregates (and thus larger ellipsometric thicknesses) are produced. As the surfactant concentration is increased, the fluorosurfactant assembled in the adsorbed aggregates tends to have a tail length that is closer to the average (bulk) chain length, and therefore the ellipsometric thickness is reduced. Evidence of such behavior has been presented in the case of adsorbed block copolymers with low polydispersity.[61]

A final general remark on the shape of the adsorption curve is in place. Close examination of the adsorption dynamics reveals that after surfactant injection some overshooting in the calculated adsorbed amount arises. Most likely this behavior is, again, related to the exchange of different surfactant species at the interface.

The adsorption isotherm shown in Figure 1b can be used for elucidation of the adsorption mechanism and the possible assembly structure. As can be seen, the resulting adsorption isotherm is characterized by three concentration regimes that, according to the classification of Giles,[62] are typical S2-type isotherms.

At low concentration the adsorption of individual molecules is driven by electrostatic attraction between the surfactant and the surface of opposite charge. In this region the surface charge density of the surface varies very little since an ion exchange process most likely occurs.

In the second regime, at a surfactant concentration below 20 μg/mL, the hydrophobic effect facilitates the association of the highly hydrophobic tails of the adsorbed fluorosurfactants, and thus the adsorbed amount increases sharply since the process is highly cooperative. The data demonstrate that bilayer aggregates start to form (in this case at a rather low surfactant concentration), and the surface charge is neutralized and later reversed by the adsorbed surfactant ions.

The last regime shows a "plateau" in the adsorbed amount as can be observed at a surfactant concentration around the cmc (30 μg/mL) or greater. We note that the adsorbed amount increases marginally, but significantly, above the cmc. We suggest that this is a consequence of attachment of some surfactant aggregates on top of the bilayer aggregates. This interpretation will be supported by the force studies presented below. At the highest surfactant concentration studied (100 μg/mL) the area

(59) Mengyang, L.; Acero, A.; Huang, Z.; Rice, S. *Nature (London)* **1994**, *367*, 151.
(60) Eastoe, J.; Downer, A.; Paul, A.; Steytler, D. C.; Rumsey, E.; Penfold, J.; Heenan, R. K. *Phys. Chem. Chem. Phys.* **2000**, *2*, 5235.
(61) Schillén, K.; Claesson, P. M.; Malmsten, M.; Linse, P.; Booth, C. *J. Phys. Chem. B* **1997**, *101*, 4238.
(62) Giles, C. H. In *Anionic Surfactants. Physical Chemistry of Surfactant Action*; Lucassen-Reynders, E. H., Ed.; Marcel Dekker: New York, 1981; Vol. 11, p 143.

per adsorbed molecule, calculated from the average surfactant structure, is significantly larger than what would be expected for a complete bilayer. Hence, not even at this concentration is the surface covered by a complete bilayer but rather bilayer aggregates are present.

Following AFM imaging studies, it has been proposed that the dominant structure of single-chain anionic (SDS) and cationic surfactants (CTAB and TTAB) adsorbed on mineral oxides surfaces (titanium dioxide, kaolinite, and quartz) is predominantly spherical or globular surface micelles.[63] Ellipsometric studies have also indicated the adsorption of $C_{12}E_6$, TTAB, and ABS on titania in the form of finite size aggregates.[64] Surface interaction force measurements, on the other hand, suggest the formation of CTAB patches of bilayers adsorbed on glass.[65] Even though it cannot be stated at this moment which type of structure assembles in the present case, the data presented later on strongly indicates the formation of (fragmented) bilayer assemblies. The formation of large fluorosurfactant aggregates (linear or ring micelles or fractal aggregates) observed in bulk solution[66,67] supports the possibility that bilayer-like structures are formed at solid interfaces. This will be investigated more closely in a coming publication.

If a structure in the form of bilayer aggregates is admitted, then it can be pictured as an arrangement where the region closest to the surface is composed of fluorosurfactant headgroups followed by a tail region and then another headgroup region facing the bulk aqueous solution. In this situation it is possible that additional (loose) attachment of surfactant assemblies onto the surface coated by bilayer aggregates takes place.

Surface Interaction Forces. In MASIF and SFA experiments the adsorption takes place on a pair of solid surfaces (glass for MASIF and mica for SFA). Thus, in the surface force studies it is possible to explore not only the effect of adsorption on the interaction forces between the two surfaces but also dynamic phenomena that occur in the adsorbed surfactant layer(s) as the interacting surfaces are moved with respect to each other.

We begin discussing a typical MASIF force curve for a fluorosurfactant-free solution. Figure 2 shows a semilogarithmic plot of the interaction force normalized by radius as a function of surface separation of glass spheres across aqueous 0.1 mM NaI solution. The force−distance relationship for this 1:1 electrolyte is in excellent agreement with the anticipated DLVO profile (down to a separation of about 5 nm) with a Debye length equivalent (within less than 5%) to that calculated from the ionic strength of the solution. At smaller separation, however, an additional repulsion is present that supersedes the expected van der Waals attraction. This short-range repulsive force between glass or silica surfaces in aqueous solutions has been reported previously,[68−70] and its origin is rationalized in terms of the dehydration of polar silanol groups (hydration force)[71] or to the compression of short polysialic acid chains (steric repulsion).[68] The apparent surface potentials at large separations and area per surface

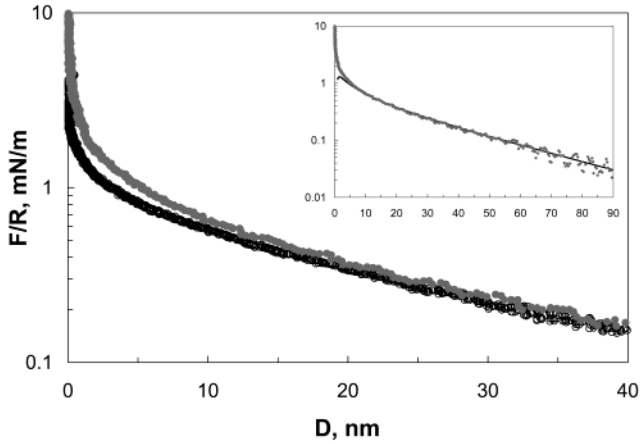

Figure 2. Semilogarithmic plot of the interaction force normalized by radius as a function of surface separation of glass spheres across aqueous 0.1 mM NaI solution (gray circles) and across 2 μg/mL fluorosurfactant solution (0.1 mM NaI background electrolyte) (black circles). In both cases no hysteresis was observed. In the inset the first curve is shown together with a fit to DLVO theory with constant surface charge boundary condition (solid line). The following parameters were used in the fitting: apparent surface potential $\Psi_0 = -86$ mV; inverse Debye length $\kappa^{-1} = 29$ nm; area per unit charge = 49.9 nm^2/charge, and Hamaker constant $A = 0.7 \times 10^{-20}$ J. Data were collected with the bimorph surface force apparatus (MASIF) at 22 °C.

charge extracted from the fitting assuming constant surface charge boundary conditions were −86 mV and 49.9 nm^2.

In the same figure the approach and separation curves measured across a 2 μg/mL fluorosurfactant solution (0.1 mM NaI background electrolyte) are included. As can be seen, there is very little change in the force profile at such low surfactant concentration. However, a reduction in the short-range repulsion is noticed. This change is a consequence of some adsorption of cationic surfactant molecules on the negatively charged glass surface. It is possible that an increase in fluorosurfactant adsorption takes place as the surface separation is reduced. However, the adsorption must by very low since the magnitude of the double-layer force hardly is affected. Corroboration of this observation is found in the ellipsometry measurements. On separation no adhesion between the surfaces was observed.

As can be seen in Figure 3, addition of fluorosurfactant up to a concentration of 10 μg/mL resulted in a dramatic change in the surface force profile. A short time (about 2 h) after the fluorosurfactant addition the long-range repulsive double-layer force initially observed disappears due to the neutralization of the surface charge by the adsorbed molecules. As has been discussed before from ellipsometric measurements, it is proposed that at this concentration surfactant (bilayer) aggregates adsorb on the surfaces. As the surfaces are brought closer, the spatial constrain causes the surfactants to adopt a structure typical of a (patchy) monolayer on each surface. As the surfaces are at molecular separations, the polar groups of the surfactant face the solid surfaces and the tails face the intervening medium and tails of surfactants adsorbed on the other surface. It is possible that under this condition the surfactant layers are not necessarily ordered, but some intercalation may occur.

Such assembly and structural rearrangement promote the attraction between the approaching surfaces, due to a combination of electrostatic attraction between positively and negatively charged patches and hydrophobic interaction. This attractive force (at separations below 12−13

(63) Schulz, J. C.; Warr, G. G. *Langmuir* **2002**, *18*, 3191.
(64) Luciani, L.; Denoyel, R. *Langmuir* **1997**, *13*, 7301.
(65) Rutland, M. W.; Parker, J. L. *Langmuir* **1994**, *10*, 1110.
(66) Oelschlaeger, C.; Waton, G.; Buhler, E.; Candau, S. J.; Cates, M. E. *Langmuir* **2002**, *18*, 3076.
(67) Giulieri, F.; Krafft, M. P. *Colloids Surf. A* **1994**, *84*, 121.
(68) Vigil, G.; Xu, Z.; Steinberg, S.; Israelachvili, J. *J. Colloid Interface Sci.* **1994**, *165*, 367.
(69) Yaminsky, V. V.; Ninham, B. W.; Pashley, R. M. *Langmuir* **1998**, *14*, 3223.
(70) Ducker, W. A.; Senden, T. J. *Langmuir* **1992**, *8*, 1831.
(71) Chapel, J.-P. *Langmuir* **1994**, *10*, 4237.

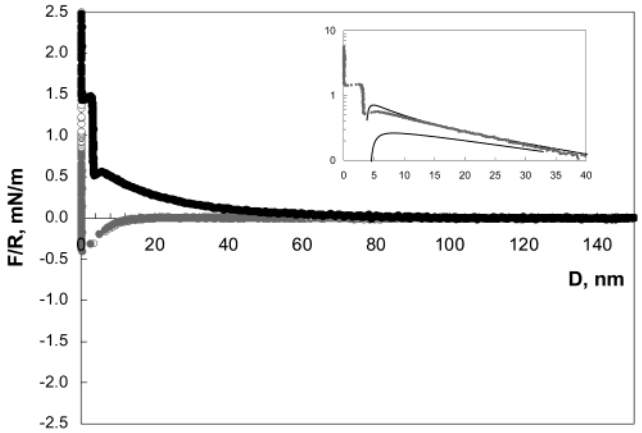

Figure 3. Force normalized by radius as a function of surface separation of glass spheres across aqueous 10 μg/mL fluorosurfactant solution (0.1 mM NaI background electrolyte). The gray circles correspond to two approach curves for short equilibration times (ca. 2 h); the filled black circles represent the inward curve for adsorption equilibrium conditions (over 10 h equilibration time). The curves on separation are not shown, but in all cases a strong adhesion (ca. 35 mN/m) was observed. Inset: amplification of the short-range force area (semilogarithmic scale). A good fit to DLVO theory with constant surface charge boundary condition is obtained by using the following parameters: $\Psi_0 = 63$ mV; inverse Debye length $\kappa^{-1} = 30$ nm; area per unit charge = 87 nm^2/charge, and Hamaker constant $A = 0.7 \times 10^{-20}$ J (upper solid line). The lower solid line represents the fit corresponding to constant surface potential boundary condition. As predicted by the DLVO approximation, a van der Waals attraction pulls the surfaces into contact at separations of 6−4 nm. The data were collected with the bimorph surface force apparatus (MASIF) at 22 °C.

nm) is in agreement with other studies showing a comparatively short-range attraction between glass surfaces neutralized by cationic hydrocarbon surfactants.[65]

Longer adsorption times result in distinctive changes in the force curve. Data obtained after more than 10 h of equilibration are shown in Figure 3. Now, a recharging of the surfaces has occurred, and a repulsive double-layer force predominates at large separations. At shorter separations a van der Waals attraction pulls the surfaces into contact between the bilayer aggregates. This "jump" is illustrated by the straight line of data points in the distance regime 6−4 nm (see inset in Figure 3). Note that these data points do not correspond to the actual force but is due to the instability of the force measuring spring. In fact, the real force is more attractive, and the adhesion between the bilayer aggregates is found to be about 1 mN/m. At shorter separations a steeply rising force is observed. This force originates from dehydration and compression of the bilayer aggregates. At a sufficiently high load, about 1.5 mN/m, the bilayer aggregates rearrange and some surfactants may leave the gap between the surfaces. This results in a second "jump" from about 3 nm to zero distance, defined here as contact between presumably patchy surfactant monolayers. The adhesion between the surfaces at this separation is 35 mN/m.

This adhesion is due to contact or interaction of the tails of the monolayers assembled on each surface. Furthermore, the adhesion between the surfaces in surfactant solutions is low compared to the case of more homogeneous surfactant monolayer coatings (e.g., from LB studies an adhesion in the range 200−300 mN/m is reported[46]), indicating in the present case low surfactant surface density in the monolayer.

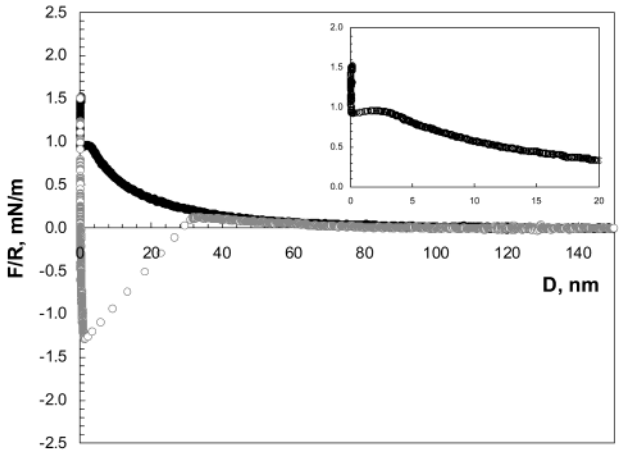

Figure 4. Force normalized by radius as a function of surface separation of glass spheres across aqueous 20 μg/mL fluorosurfactant solution (0.1 mM NaI background electrolyte). The filled black circle curve represents the approach curve for adsorption equilibrium conditions, and the gray circles curve corresponds to the separation (outward) run after adsorption equilibrium. On separation an adhesion of about 1.5 mN/m was observed. Inset: amplification of the short-range force area. The data were collected with the bimorph surface force apparatus (MASIF) at 22 °C.

An increase in the surfactant concentration to 20, 50, and 100 μg/mL generated the surface force interactions illustrated in Figures 4, 5, and 6, respectively. Figure 4, for the 20 μg/mL fluorosurfactant concentration, is qualitatively similar to the 10 μg/mL situation. However, in this particular case a low load was exerted (maximum force equivalent to 1.5 mN/m) before the surfaces were retracted. Thus, only the first (outermost) jump was observed, i.e., that resulting from van der Waals forces between the surfaces (partially) coated with bilayer aggregates. The measured adhesion is that corresponding to a bilayer−bilayer contact, which amounts to about 1.3−1.4 mN/m, compared to ca. 25 mN/m observed when the outer layer is pressed out. The lower value of the adhesion between bilayer aggregates (compared to the monolayer−monolayer contact) is expected since in this situation surfactant headgroups rather than tails cover the majority of the external areas.

For the 50 and 100 μg/mL cases (Figures 5 and 6, respectively) even at the highest applied loads (about 10 mN/m) it was not possible to measure strong adhesion forces (as those typical of monolayer−monolayer contact). This fact indicates that at these concentration levels the bilayer is more fully formed on the surfaces, and it becomes impossible to force out the surfactants in the outer surface layer under the experimental loads. In both cases the hard-wall contact corresponds to the thickness of a bilayer and the pull-off measured on separation is that of bilayer−bilayer contact which is about 2.4 and 2 mN/m for the 50 and 100 μg/mL cases, respectively.

Since the separation calculated in the MASIF operation is relative to that of a hard-wall contact (the actual position with respect to zero distance is usually not known), we have redrawn Figures 3−6 in a master plot (see Figure 7) with a correction of the distance scale based on the layer structure information gathered from ellipsometry and SFA results to be presented below.

From Figure 7 some issues are worth noting. First, at 10 μg/mL surfactant concentration it is relatively easy to reach the monolayer−monolayer contact. In this situation a strong adhesion is measured. At 20 μg/mL, on the other hand, both bilayer−bilayer and monolayer−monolayer

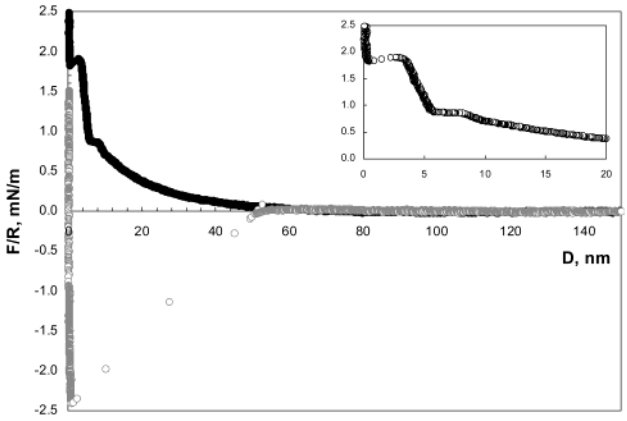

Figure 5. Force normalized by radius as a function of surface separation of glass spheres across aqueous 50 μg/mL fluorosurfactant solution (0.1 mM NaI background electrolyte). The filled black circle curve represents the approach curve for adsorption equilibrium conditions, and the gray circles curve corresponds to the separation (outward) run after adsorption equilibrium. On separation an adhesion of about 2.5 mN/m was observed. Inset: amplification of the short-range force area. The data were collected with the bimorph surface force apparatus (MASIF) at 22 °C.

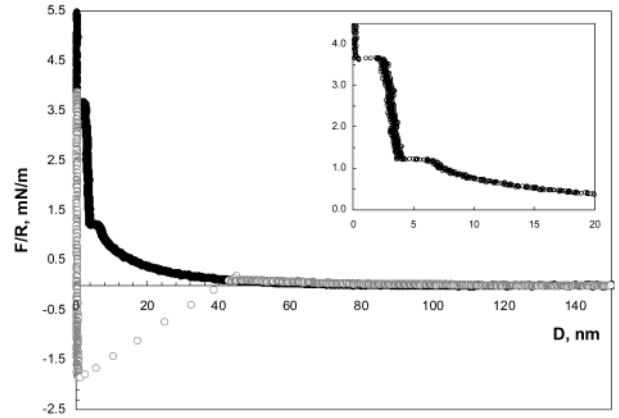

Figure 6. Force normalized by radius as a function of surface separation of glass spheres across aqueous 100 μg/mL fluorosurfactant solution (0.1 mM NaI background electrolyte). The filled black circle curve represents the approach curve for adsorption equilibrium conditions, and the gray circles curve corresponds to the separation (outward) run after adsorption equilibrium. On separation an adhesion of about 1.7 mN/m was observed. Inset: amplification of the short-range force. The data were collected with the bimorph surface force apparatus (MASIF) at 22 °C.

contact are attainable (only the first situation is depicted). For concentrations of 50 μg/mL or higher only bilayer−bilayer contact is reached (under the exerted loads of typically 10 mN/m or less). Second, the force load required to achieve bilayer−bilayer contact increases as the surfactant concentration is increased. Above the cmc of the surfactant (30 ppm), an additional force barrier (in excess of that crated by electrostatic double-layer forces) is observed outside bilayer−bilayer contact. We attribute this barrier to surfactant aggregates associated with the bilayer-coated surface. Third, the distance jump from bilayer contact to monolayer contact corresponds to a distance of ca. 3 nm. This distance, as shown by ellipsometry experiments, corresponds to the thickness of a bilayer. A similar figure (3.3 nm) was obtained for bilayers formed by cetyltrimethylammonium bromide (CTAB) on mica at a bulk concentration of about one-half the critical micelle concentration.[72]

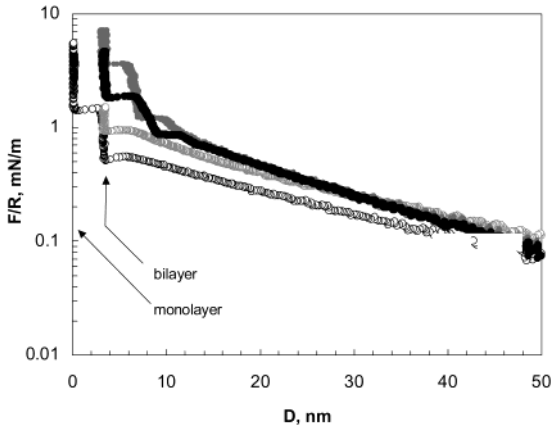

Figure 7. Summary of force curves (semilog scale) for glass spheres across fluorosurfactant solution of 10 (open black circles), 20 (open gray circles), 50 (filled black circles), and 100 μg/mL (filled gray circles) concentrations (0.1 mM NaI background electrolyte). All the curves correspond to the approach (or inward) runs. The hard-wall or constant compliance zones are located at different zero distance depending on the occurrence of bilayer−bilayer or monolayer−monolayer contact. Observe that the forces required to overcome the force barrier are higher as the surfactant concentration is increased. The data were collected with the bimorph surface force apparatus (MASIF) at 22 °C.

Since in the bilayer aggregates the surfactant chains are probably partially intercalated, the actual length of the adsorbed surfactant molecules should be about 1.5 nm or higher. A rough calculation using the relationship for the calculation of a surfactant tail length is presented in ref 73; an equivalent hydrocarbon chain for the studied surfactant yields a fully (maximum) length (L_{max}) of 1.8 nm, and thus a bilayer thickness of about $1.6L_{max} = 2.9$ nm is expected. As can be seen, the obtained results fit very well the idea of an adsorbed assembly in the form of a bilayer aggregate. We note that neutron reflection studies of adsorbed monolayers of decyl- and hexadecyltrimethylammonium bromide at the air/liquid interface showed a layer thickness of 1.7 and 2.1 nm, respectively.[74] Values in the range of 1.1−2 nm according to space-filling models of a fluorosurfactant similar to the one studied here are reported in refs 75 and 76 for various surface conformations.

Figure 8 summarizes the adhesion, or pull-off force, for different surfactant concentrations. As discussed in previous paragraphs, two cases are distinguished: adhesion between patchy monolayer−monolayer and between patchy bilayer−bilayer contacts. In the first case a stronger adhesion is present, whereas in the second case (bilayer−bilayer contact) the adhesion is much smaller and roughly independent of the concentration. The load required to reach bilayer−bilayer contact is also plotted on the positive side of the graph, and it is evident that an increased load is required as the fluorosurfactant concentration is increased. This is due to a combination of repulsive double-

(72) Kékicheff, P.; Christenson, H. K.; Ninham, B. W. *Colloids Surf.* **1989**, *40*, 31.
(73) Evans, D. F.; Wennerström, H. *The Colloidal Domain: Where Physics, Chemistry, Biology, and Technology Meet*, 2nd ed.; Wiley-VCH: New York, 1999.
(74) Ingram, B. T.; Ottewill, R. H. In *Cationic Surfactants: Physical Chemistry*; Rubingh, D. N., Holland, P. M., Eds.; Marcel Dekker: New York, 1991; Vol. 37, p 87.
(75) Gerenser, L. J.; Pochan, J. M.; Mason, M. G.; Elman, J. F. *Langmuir* **1985**, *1*, 305.
(76) Gerenser, L. J.; Pochan, J. M.; Elman, J. F.; Mason, M. G. *Langmuir* **1986**, *2*, 765.

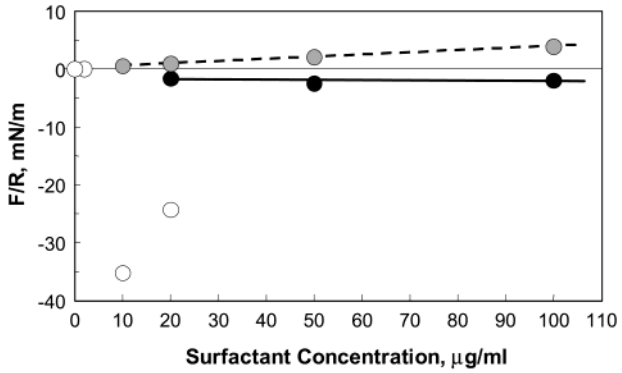

Figure 8. Adhesion forces between glass spheres covered by surfactant assemblies produced after reaching monolayer−monolayer contact (open circles) or bilayer−bilayer contact (filled black circles) for different fluorosurfactant concentrations. These adhesion forces are, as conventionally done, displayed in the negative side of the diagram. The normalized force load required to reach bilayer−bilayer contact (gray filled circles) is also included in the positive side of the plot. The data were collected with the bimorph surface force apparatus (MASIF) at 22 °C.

layer forces and, above cmc, loosely bound surfactant aggregates.

Since an absolute quantification of the distance in the force profile is desirable to test the conclusions drawn from the MASIF experiments, an attempt was made to reproduce the force curves using the interferometric surface force apparatus (Mark IV SFA). It should be noted that in this case the solid surfaces consist of mica and the geometry was that of crossed cylinders (rather than two glass spheres as in the MASIF).

As such, Figure 9 presents the force profiles, determined both on approach and on separation, for surfactant concentrations of 10 and 25 μg/mL. Even though the background electrolyte is different, some key features are common to the cases presented previously. At 10 μg/mL concentration the layer thickness (as illustrated by the hard wall profile) is 3−4 nm, which is identical to the MASIF result for the thickness of a bilayer. At 25 μg/mL the hard-wall distance (for low force loads) is about 6−9 nm, which corresponds to about twice the value found for a bilayer as before. Therefore, in this case bilayer aggregates are formed on each surface. Even at the highest applied load (5 mN/m) it was not possible to drive out the outer surfactant layers, and a higher force would be required to reach monolayer−monolayer contact. In fact, it has been reported that after the formation of a surfactant bilayer on mica it becomes impossible to push the two surfaces into strong hydrophobic contact (as opposed to the case of glass surfaces).[65] It can also be noted that in the case of monolayer−monolayer contact (10 μg/mL) the adhesion measured on separation is higher than the adhesion for bilayer−bilayer contact (25 μg/mL case), i.e., 24 and 2 mN/m, respectively.

A comparison of the MASIF and SFA pull-off forces is not straightforward. However, some assessment can be made considering that the measured F/R for MASIF (spheres) experiments is related to the interaction free energy per unit area (G) between parallel plates of unit area by $F/R = \pi G$ whereas in the case of the SFA (cross-cylinder geometry) F/R scales as $F/R = 2\pi G$, and therefore the relationship $(F/R)_{SFA} = 2(F/R)_{MASIF}$ is expected to hold for the measured interaction forces. As can be seen, in the case of the highest pull-off forces (monolayer−monolayer adhesion), the experimental values do not conform to this correlation (the adhesion values are relatively similar for

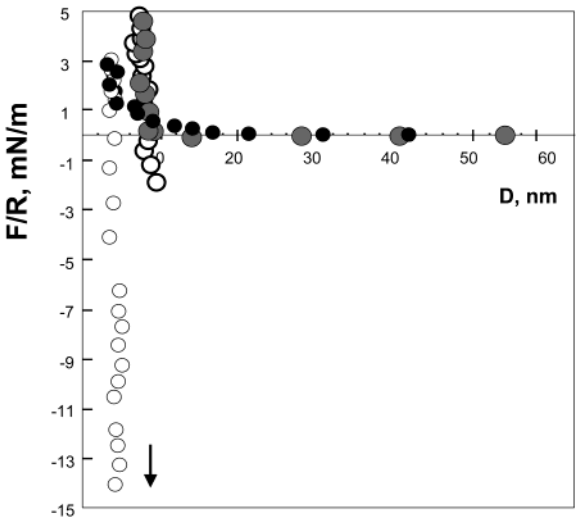

Figure 9. Force normalized by radius of mica surfaces in crossed cylinder geometry as a function of surface separation across aqueous 10 and 25 μg/mL fluorosurfactant solutions (0.05 M PBS buffer as background electrolyte). The filled black circle curve represents the approach curve for adsorption equilibrium conditions for 10 μg/mL concentration and the filled gray circle for 25 μg/mL concentration. The open circle curves correspond to separation (outward) runs after adsorption equilibrium for the same concentrations, i.e., 10 μg/mL (open circle) and 25 μg/mL (open bold circles). On separation an adhesion of about 2 mN/m was observed for 25 μg/mL fluorosurfactant concentration. For the 10 μg/mL surfactant concentration case the observed pull-off force was 24 mN/m (scale in the plot is shortened and thus the data point is not depicted). In the 10 μg/mL approach curve a jump of about 3 nm is observed (at a force load of ca. 1 mN/m). Also, the absolute hard-wall distance is about 6 nm for the 10 μg/mL inward run and about 12 nm for the 25 μg/mL inward run. The data were collected with a Mark IV interferometric surface force apparatus at 22 °C.

MASIF and SFA, i.e., 35 and 24 mN/m, respectively). This indicates that the packing of the surfactant layers is somewhat different on the two surfaces. This has also been observed for e.g. CTAB.[65] The difference in ionic strength in the MASIF and SFA experiments may also affect the adhesion values.

The adhesion measured by the SFA for fluorosurfactants deposited on mica by LB techniques is much higher. An adhesion of 200−300 mN/m (equivalent to 100−150 mN/m for the MASIF) was reported for a double-chain cationic fluorosurfactant.[46] There are several reasons for this. During LB deposition all molecules are initially oriented with the charged group toward the surface. With time some rearrangements may occur with some molecules in the monolayer changing orientation or moving to form an outer layer. Such rearrangements are counteracted by the electrostatic affinity between the surfactant and the surface but promoted by a striving to reduce the interfacial tension toward water. On the other hand, for the surfactant adsorbing from solution the layer structure formed initially consists of bilayer aggregates. In the confined space between the surfaces a rearrangement into a patchy monolayer structure is proposed. Clearly, the difference in adhesion force measured between LB monolayers and adsorbed "monolayers" is a strong indication that the latter are significantly less hydrophobic. The reasons for this can be less surface coverage and more surfactant head-groups pointing outward, or a combination of the two. We also note that vapor cavities form between LB monolayers in contact whereas no such cavities were observed in the present case. This confirms the lower hydrophobicity of the "monolayer" contact for adsorbing fluorosurfactants.

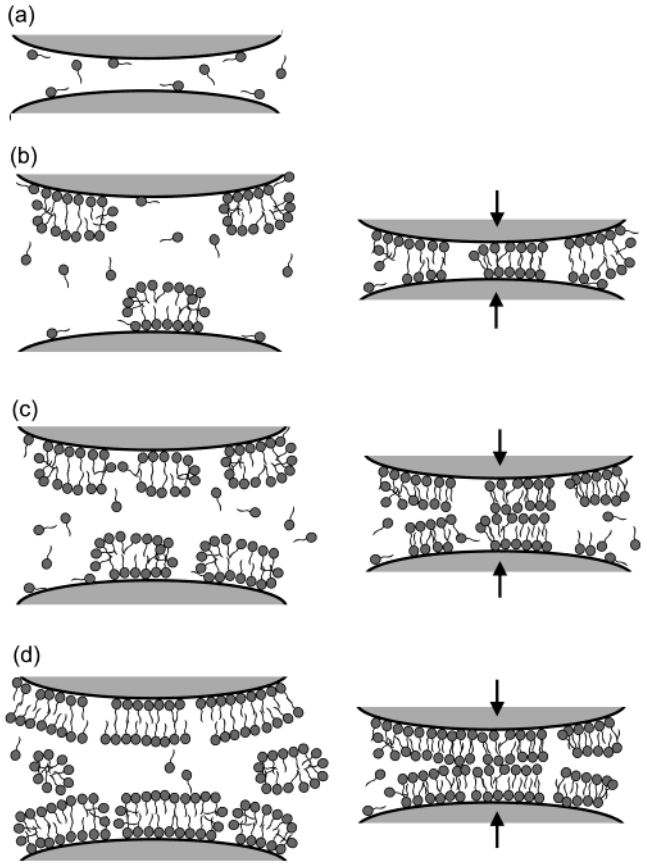

Figure 10. llustration of the hypothesized assembly of fluorosurfactants adsorbed on two approaching surfaces (as those in the MASIF or SFA experiments) for surfactant concentrations of 2 μg/L (a), 10 μg/L (b), 20 μg/L (c), and 50 μg/L or higher (d). The situation for large separations and when the surfaces are in contact are illustrated on the left and right side of the figure, respectively.

In general, the SFA results supports the description advanced from the MASIF experiments. An illustrative scheme of the structure of the surfactant assemblies on the (approaching) surfaces is presented in Figure 10. At 10 and 20 μg/mL few bilayers aggregates are formed, and monolayer−monolayer contact is relatively easy to reach. In this case there is a strong adhesion. For 50 μg/mL or higher, more bilayers aggregates are formed, and monolayer−monolayer contact is difficult (impossible) to reach. In this situation the measured adhesion corresponds to bilayer−bilayer contact which, compared to monolayer−monolayer contact, is at least 1 order of magnitude smaller. The structures drawn in the gap for high-concentration conditions represent aggregates of fluorosurfactant molecules.

Let us for a moment consider similarities and differences between cationic hydrocarbon surfactants and cationic fluorocarbon surfactants adsorbing to glass and their effect on surface forces. Some basic facts are that the electrostatic affinity of the surfactants to the surface is the same whereas the fluorocarbon chain is more hydrophobic than the hydrocarbon chain. Relevant data to compare our results with are presented in refs 65 and 77 which deal with CTAB adsorption on glass.

At pH 5.7 adsorption of CTAB close to neutralize the surface charge at a surfactant concentration of 0.046 mM, i.e., at a concentration corresponding to 5% of the cmc. For the fluorosurfactants studied here charge neutralization never occurs at equilibrium. At 2 μg/mL (6% of the cmc) the adsorption is very limited. At 10 μg/mL concentration (0.3 cmc) charge neutralization is achieved, but only temporarily, and a strong recharging occurs with time due to formation of bilayer aggregates. Clearly, the stronger hydrophobicity of the fluorocarbon chain makes adsorption into monolayer aggregates less favorable since the interfacial tension toward water would be higher. Instead, we observe that bilayer aggregates form readily once the surface density of adsorbed surfactants has reached a critical level. In contrast, the buildup of bilayer aggregates for CTAB on glass appears to occur more gradually. We note that in both cases bilayer aggregates that are difficult to transform into monolayer aggregates under compression are present on the surfaces at close to half the cmc.

Conclusions

Ellipsometric and surface force experiments indicate that cationic fluorosurfactants self-assemble on solid surfaces (silica, glass, and mica) in the form of bilayer structures. This process takes place at rather low surfactant concentration and explains the improvement in separation efficiency and peak symmetry reported in the literature when fluorosurfactants are used in capillary electrophoresis.

Adsorption of fluorosurfactants on solid surfaces influences the interaction forces between the adsorbed layers quite dramatically. At low fluorosurfactant concentration the molecules adsorb both on glass and mica surfaces due to favorable electrostatic interactions. At higher surfactant concentrations hydrophobic interactions continue to drive the adsorption process.

Contrary to the long-range interactions observed between LB-deposited monolayers of fluorosurfactants, the interaction forces for fluorosurfactants adsorbed directly from solution is dominated by a repulsive component emerging from adsorbed bilayer aggregates. No long-range "hydrophobic" attractions are observed, and for low surfactant concentration a "jump-in" (or force instability) at high loads is observed which is explained by a transformation of bilayer aggregates on the isolated surfaces to monolayer aggregates on each surface when their separation is small. At higher concentrations it is difficult (impossible) to reach monolayer−monolayer contact, and bilayer−bilayer contact is observed. In this case the resulting energy of adhesion is an order of magnitude lower than for monolayer−monolayer contact.

It was demonstrated that the structures that start to build up on solid surfaces at low fluorosurfactant concentration (e.g., 10 μg/mL) are dependent on the incubation time and that the associated interaction forces evolve accordingly. At higher concentration bilayer aggregates adsorbed on the surface are likely to occur, and molecular rearrangement arises as the surfaces come in contact.

The force load required to reach bilayer−bilayer contact increases with the fluorosurfactant bulk concentration, and the resulting bilayers have low adhesion energies. Also, the adhesion between the surfaces when pushed into "monolayer" contact in surfactant solutions is low as compared to the values reported for uniform/full surfactant coverage, indicating therefore low aggregate packing density.

The thickness of the adsorbed bilayer aggregates is ca. 3 nm. The measured thickness is reduced slightly as the surfactant concentration is increased, and it is hypothesized that this is due to the surfactant's size polydis-

(77) Parker, J. L.; Yaminsky, V. V.; Claesson, P. M. *J. Phys. Chem.* **1993**, *97*, 7706.

persity. The adsorbed amount at equilibrium on silica in contact with a 100 μg/mL fluorosurfactant solution is about 2.9 mg/m^2, which is equivalent to a specific area of ca. 84 Å^2 per molecule, which agrees with a patchy or incomplete coverage. In summary, our data strongly support the formation of fragmented bilayer aggregates of fluorosurfactants when they are adsorbed on hydrophilic surfaces directly from aqueous solution.

Acknowledgment. Financial support from the Strategic Research Foundation (SSF) programs "Nanochemistry" and "Colloid and Interface Technology" is acknowledged. O.J.R. thankfully acknowledges financial support from FONACIT and CDCHT-ULA.

LA025989C